



## Adsorption of Naphthol Blue Black Dye onto Acid Activated Titania Pillared Bentonite: Equilibrium Study

SURYA LUBIS\*, SHEILATINA, SYAHRINTA SEPIA NIKA and VICKY PRAJA PUTRA

Department of Chemistry, Faculty of Mathematics and Natural Sciences,  
Syiah Kuala University, Darussalam, Banda Aceh 23111, Indonesia.

\*Corresponding author E-mail: suryalubis@unsyiah.ac.id

<http://dx.doi.org/10.13005/ojc/320407>

(Received: June 10, 2016; Accepted: July 25, 2016)

### ABSTRACT

The synthesis of acid activated titanium dioxide-pillared bentonite ( $\text{TiO}_2$ -pillared bentonite) and its adsorption properties on naphthol blue black (NBB) dye has been studied. Natural bentonite was activated by using hydrochloric acid solutions and was intercalated with tetraisopropyl orthotitanate as titanium dioxide precursor. The as-prepared materials were characterized by X-ray Diffraction (XRD), nitrogen adsorption-desorption isotherms and Scanning Electron Microscopy Energy Dispersive X-ray Analysis (SEM-EDX). Naphthol blue black dye removal was seen to increase with increasing contact time and the adsorption capacity of acid activated  $\text{TiO}_2$ -pillared bentonite was depending on the pH, initial dye concentration and the amount of adsorbent. The optimum condition of NBB dye adsorption was found at a pH of 3.0, adsorbent amount of 0.2 g, initial dye concentration 25 mg/L for 120 minutes adsorption time. The adsorption capacity for the dye was found to be 1.496 mg/g. Adsorption of NBB onto  $\text{TiO}_2$ -pillared bentonite at these conditions followed the Langmuir and Freundlich isotherm but the value of the correlation coefficient of Langmuir isotherm (0.998) is higher than Freundlich isotherm value (0.952).

**Keywords:** bentonite, acid activated, pillared, naphthol blue black, adsorption.

### INTRODUCTION

Removal of dye wastewater is a major problem face in the food, pharmaceutical, cosmetics, paint, pigment, paper, printing, and textile industries. Inefficiencies in the textile dying processes result to more than 15% of the dye stuff being lost directly to wastewater<sup>1</sup>. There is a current need to treat dye-containing wastewater prior to their discharge

as these compounds and their degradation products can be toxic and carcinogenic, even at low concentrations. High concentrations of dye also impart colour to aquatic life in rivers and lakes and affect its aesthetic value<sup>2</sup>. Among these dyes is naphthol blue black (amido black 10B) is an azo dyes, characterized by the presence of at least one –N–N– group are the most widely exploited dyes in the textile industry accounting for about 70% of all

dye stuffs used<sup>3,4</sup> Cotton, rayon, and other cellulosic fibers, as well as silk, can be dyed with azoic or naphthol dyes.

Some methods have been developed to treat dye wastewater include: physical, chemical and biological processes<sup>5</sup>. Physical methods include sedimentation and filtration, while chemical methods were conducted by coagulation, flocculation, oxidation and adsorption. In comparison with other processes for the treatment of dye waste water, the adsorption process is an attractive method because adsorption allows flexibility in terms of both design and operation and produces pollutant-free effluents that are suitable for reuse. Additionally, as the adsorption is sometimes reversible, the sorbent can be regenerated, thereby resulting in significant cost savings<sup>6,7</sup>.

Several authors have reported the use of adsorbents such as activated silica, chitosan, zeolite, activated carbon, wood, fly ash and clays<sup>8</sup>. Although activated carbon remains the most widely used adsorbent, its relatively high cost restricts its use somewhat<sup>9</sup>. In addition to cost, high adsorption properties and availability are also key criteria when it comes to choosing an adsorbent for pollutant removal, thereby encouraging research into materials that are both efficient and cheap.

Bentonite, as a low cost clay, are important raw materials of choice for the novel materials because they are abundant, inexpensive and environmentally friendly<sup>10,11</sup>. Bentonite consisting mostly of montmorillonite, with permanent negative charges on its surface has been used in many applications for water treatment<sup>12,13</sup>. However, these low-cost adsorbents have a low adsorption capacity but recent studies have demonstrated that the adsorption capability can be enhanced by modification of these adsorbents via physical and enhanced chemical processes<sup>14</sup>. Bentonite can be intercalated by inorganic and/or organic cations and the resulting materials have high specific surface area associated with their small size<sup>15</sup>. Basically, the modification reactions employed herein for the preparation of modified bentonites are accomplished by replacing the interlayer cations (e.g. Na<sup>+</sup>, K<sup>+</sup>, Ca<sup>2+</sup>) with specific species (polynuclear metal species) to alter the surface and/or structural characteristics of

the clay<sup>16</sup>. The pore structure and surface chemistry of the adsorbent have the greatest influence on the adsorption process<sup>17</sup>, whereas the pore size distribution affects the efficiency and selectivity of adsorption. Several studies have been conducted to illustrate the relationship between the pore size distribution of adsorbents and their adsorption capacity<sup>18,19</sup>.

Modification of bentonite is vital for the adsorption of anionic dyes, as the net negative charge on the dye and clay surface brings charge repulsion and thus, resulting in lowering surface interaction and adsorption<sup>20,21</sup>. The charge repulsion can be decreased by intercalation of bentonite interlayer with titanium dioxide, TiO<sub>2</sub> which has amphoteric behavior<sup>21</sup>. Herein, in this study, we reported the modification of natural bentonite to acid activated and titania-pillared bentonite and determine key operating parameters: pH, adsorbent dosage, initial dye concentration and contact time on NBB adsorption. The experimental data will be evaluated by Langmuir and Freundlich adsorption isotherms.

## MATERIALS AND METHODS

The chemical used in this study, tetraisopropyl orthotitanate (Ti[OCH(CH<sub>3</sub>)<sub>2</sub>]<sub>4</sub>), naphthol blue black (amido black 10B, Fig. 1), an anionic dye with the chemical formula C<sub>22</sub>H<sub>14</sub>N<sub>6</sub>Na<sub>2</sub>O<sub>9</sub>S<sub>2</sub> (C.I. = 20470 and MW= 616.49 g/mole) were purchased from Merck. Bentonite was obtained from Kuala Dewa, North Aceh, Indonesia. Bentonite was sieved to give different particle size fractions using 100 mesh ASTM standard sieves (149 μm).

### Preparation of acid activated TiO<sub>2</sub>-pillared Bentonite

#### Acid Activation of natural bentonite

The acid activation of natural bentonite was carried out at room temperature for 24 hours. Natural bentonite was treated with 1.0 M aqueous hydrochloric acid and was stirred magnetically. The bentonite to acid ratio was fixed at 1:10 (g/mL). After 24 h the reaction was terminated and the mixture was filtered then was washed several times with deionised water until chloride ion was undetectable in the supernatant using silver nitrate solution. The final sample was centrifuged with centrifuge AllegraX-12, and dried at 100°C for 12 h.

### Preparation of acid activated TiO<sub>2</sub>-Pillared Bentonite

Dried acid activated bentonite (100 g) was added to 333 mL saturated sodium chloride solution and was stirring for 2 hours. The modified bentonite was separated by centrifugation followed by drying at 100°C for 12 hours. Modification was conducted by using ammonium chloride solution to obtain H-Bentonite. H-Bentonite was modified to TiO<sub>2</sub>-pillared bentonite by using titanium tetra isopropoxide with the molar ratio HCl to titanium tetra isopropoxide was 4 : 1 as pillaring agent. The pillaring agent was added to bentonite suspension (10 g bentonite in 500 mL distilled water). The mixture was stirred at room temperature for 12 h and then was separated by centrifugation. The obtained material was drying at 100°C for 12 h and was calcined at 450°C for 5 hours.

### Characterization

The specific surface area and average pore size of the natural, acid activated and TiO<sub>2</sub>-pillared bentonite samples were analyzed using, respectively, the BET and BJH methods. The determinations of the surface area and pore size were based on isotherms of adsorption and desorption of nitrogen at 77±0.5 K using a Quantachrome Nova 3200E instrument. The sample tubes were loaded with 0.1-0.2 g of bentonite samples. The samples were then degassed under vacuum at 378 ±1 K for 12 h in Vacuum prior to surface area measurements. The morphological features and surface characteristics of samples were obtained from scanning electron microscopy (SEM) using JEOL-JSM-6510LV at an accelerating voltage of 15 kV. The structure of materials were identified by a Shimadzu X-ray diffractometer (XRD) equipped with Cu K $\alpha$  radiation ( $\lambda = 0.15405$  nm 30 kV, 15 mA) and a monochromator at a 2 theta angle between 5 to 80 degrees.

### Adsorption Experiments

NBB dye was dissolved in distilled water to prepare a stock solution of 1 g/L concentration. This stock solution was diluted in order to prepare NBB solutions of concentration ranging from 5 to 25 mg/L. The calibration curve of NBB solution was obtained by measuring the absorbance of these samples at the maximum absorbance wavelength of NBB ( $\lambda_{\text{max}} = 618$  nm) using a spectrophotometer UV-Vis (Shimadzu UV mini 1240).

The adsorption experiments were performed in batch experiments at room temperature in 100 mL conical Erlenmeyer flask containing 25 mL of NBB solution. The flasks were wrapped in aluminium foil and were placed in a shaker (Memmert type SV 1422) with a shaking speed of 150 rpm. Samples were collected at determined time intervals, then centrifugal separation at 1000 rpm for 15 minutes using Centrifuge Hettch-EBA III. The colour removal was analyzed by calculating the concentration of NBB (mg/L) by using a standard calibration graph.

Batch pH studies were carried out by shaking 25 mL of 15 mg/L NBB solution with 0.2 g of acid activated TiO<sub>2</sub>-pillared bentonite. The pH of the solutions was adjusted with HCl or NaOH solution and measured by using a pH meter. In this experiment, five different sample dosages (0.2; 0.4; 0.6; 0.8 and 1 g) were selected to study the adsorption of NBB onto acid activated TiO<sub>2</sub>-pillared bentonite. The experiments were performed at optimum pH obtained from above experiment for 0 - 120 minutes.

In the determination of equilibrium adsorption isotherm and adsorption kinetics, an optimum amount of acid activated TiO<sub>2</sub>-pillared bentonite obtained from above experiment and NBB solution with the initial concentration 5–25 mg/L were transferred in 100 mL flask, shaken with a shaking speed of 150 rpm for 0 – 120 minutes. The pH of NBB solution was adjusted at optimum pH obtained from prior experiment.

### Adsorption Equilibrium

The amount of dye adsorbed or the equilibrium adsorption capacity,  $q_e$  (mg/g) at equilibrium were calculated from the following equation:

$$q_e = (C_o - C_e) \frac{V}{m} \quad \dots(1)$$

Adsorption isotherm of NBB was fitted by the Langmuir and Freundlich models using linearised parameter estimations. The linear form of Langmuir isotherm is [22]:

$$\frac{C_e}{q_e} = \frac{1}{K_L} + \frac{a_L}{K_L} C_e \quad \dots(2)$$

where,  $q_e$  (mg/g) is the amount of adsorbate adsorbed on unit mass of adsorbent,  $C_o$  and  $C_e$  (mg/L) are the initial and equilibrium concentration of NBB in solution,  $V$  (L) is the solution volume and  $m$  (g) is the mass of the  $TiO_2$ -pillared bentonite.  $K_L$  (L/g) is the Langmuir equilibrium constant and  $K_L/a_L$  give the  $Q_o$  (mg/g) the theoretical monolayer saturation capacity. The  $K_L$  and  $a_L$  values were calculated from the intercept and slope of the straight line obtained after plotting  $C_e/q_e$  against  $C_e$ , respectively.

The Langmuir isotherm was further evaluated by the dimensionless constant called separation factor ( $R_L$ , equilibrium parameter) which is defined by the following equation:

$$R_L = \frac{1}{1 + a_L C_o} \quad \dots(3)$$

with,  $C_o$  (mg/L) is the initial adsorbate concentration and  $a_L$  (L/mg) is the Langmuir constant related to the energy of adsorption. The value of  $R_L$  indicates the shape of the isotherms to be either unfavorable ( $R_L > 1$ ), linear ( $R_L = 1$ ), favorable ( $0 < R_L < 1$ ) or irreversible ( $R_L = 0$ ) [23].

The linear form of Freundlich isotherm isotherms is:

$$\log q_e = \log K_F + \frac{1}{n} \log C_e \quad \dots(4)$$

where  $K_F$  ( $mg^{1-1/n}L^{1/n}/g$ ) is the Freundlich constant and  $n$  (g/L) is the Freundlich exponent. A plot of  $\log q_e$  versus  $\log C_e$  enables the constant  $K_F$  and exponent  $n$  to be determined.

## RESULTS AND DISCUSSION

### Characterization of the adsorbent

The XRD analysis showed that natural bentonite from Kuala Dewa, North Aceh Indonesia consisted of montmorillonite, quartz, feldspar and calcite (Fig. 2). The natural bentonite was classified as Ca-bentonite due to the chemical composition of bentonite was  $Fe_2O_3$  (10.29%),  $ZnO$  (3.89%),  $MgO$  (1.86),  $Al_2O_3$  (25.36%),  $SiO_2$  (55.76%),  $K_2O$  (1.25%),  $CaO$  (1.23%),  $TiO_2$  (0.36%) and no sodium ion was detected. Fig. 2 shows that there is no significant differences between XRD patterns of natural bentonite and  $TiO_2$ -pillared bentonite. The difference was confirmed at small angle diffractogram. Fig. 3 shows the small  $2\theta$  ( $5-10^\circ$ ) angle XRD patterns of the natural bentonite and  $TiO_2$ -pillared bentonite. A typical diffraction peak of natural Bentonite at  $5.69^\circ$  corresponds to a basal spacing of 2.51 nm. The XRD pattern of  $TiO_2$ -pillared Bentonite does not contain a (001) diffraction, indicating a highly disordered structure. The disordered structure might be due to the non-uniform interlayer distances in the bentonite which are results of inhomogeneous intercalation by small-sized Ti hydrolyzed species<sup>24</sup>.

The interactions between adsorbates and adsorbents determined the adsorption process of dye molecule on the surface of materials. Likewise, the physical characteristics of the adsorbent allow the access of molecules to the pores inside the porous material. The accessible adsorbent surface is therefore especially important in the adsorption processes<sup>7</sup>. The nitrogen adsorption-desorption isotherms of the natural, acid activated bentonite and  $TiO_2$ -pillared bentonite at 77 K are shown in Fig. 4. It can be seen that all the isotherms are the

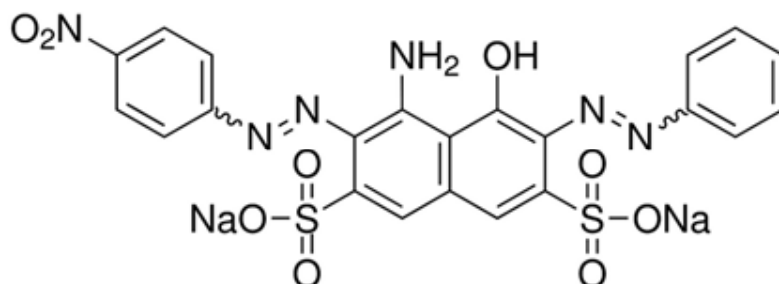


Fig. 1: Naphthol blue black BB (4-Amino-5-hydroxy-3-[(4-nitrophenyl)azo]-6-(phenylazo)-2,7-Naphthalene disulfonic acid, disodium salt)

characteristic type IV solid, indicating that the pore size in the mesopore range (IUPAC classification,<sup>25</sup>. The total pore volume of samples obtained from the Barret–Joyner–Halender (BJH) equation did not shown significant differences. The specific surface area of acid activated bentonite was higher than that of natural bentonite, while the specific surface area of TiO<sub>2</sub>-pillared bentonite was slightly decreased compare with acid activated bentonite.

Fig. 5. shows SEM images of natural bentonite and TiO<sub>2</sub>-pillared bentonite. The natural bentonite shows larger particles, whereas smaller particles and agglomerates and disordered structures were detected in TiO<sub>2</sub>-pillared bentonite. The amount of TiO<sub>2</sub> on the samples measured by SEM-EDX analysis showed 0.36 wt% on the natural bentonite and 2.58% in TiO<sub>2</sub>-pillared bentonite.

**Table 1: Specific surface areas, total pore volume and average pore diameter of the adsorbents**

Sample	S <sub>BET</sub> (m <sup>2</sup> /g)	V <sub>t</sub> (cm <sup>3</sup> /g)	Average pore diameter (nm)
Na <sub>2</sub> -Bentonit	15.880	0,042	10,740
H-Bentonite	20.540	0,033	6.618
TiO <sub>2</sub> -Bentonit	19.670	0,042	8.620

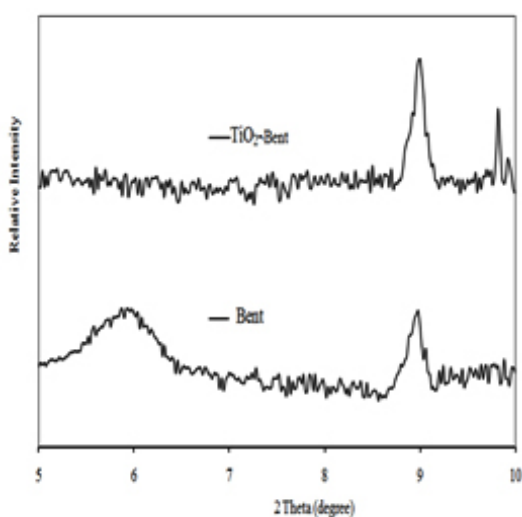


**Fig. 3: Small angle XRD pattern of Ca-Bentonit and TiO<sub>2</sub>-Bentonite**

## Adsorption Properties of Acid Activated TiO<sub>2</sub>-Pillared Bentonite

### Effect of pH on adsorption capacity

The pH of dye solution plays an important role because it may promote or suppress dye uptake by influencing not only the surface charge of the adsorbent, the dissociation of functional groups on the active sites of the adsorbent but also the solution dye chemistry<sup>26, 27</sup>. The hydrogen and hydroxyl ions are adsorbed quite strongly, and therefore, the adsorption of other ions is affected by the pH of the solution. It is a commonly known fact that the anions are favorably adsorbed by the adsorbent at lower pH

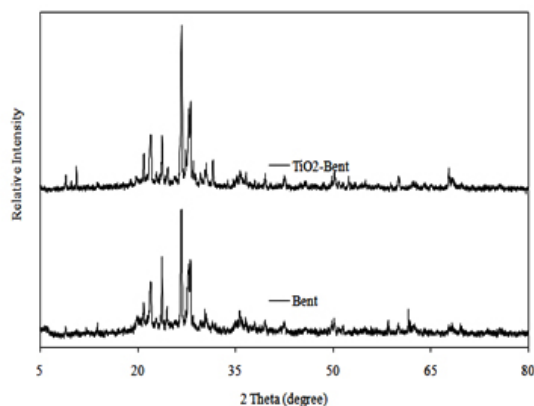


**Fig. 2: XRD pattern of natural bentonit and TiO<sub>2</sub>-pillared bentonite**

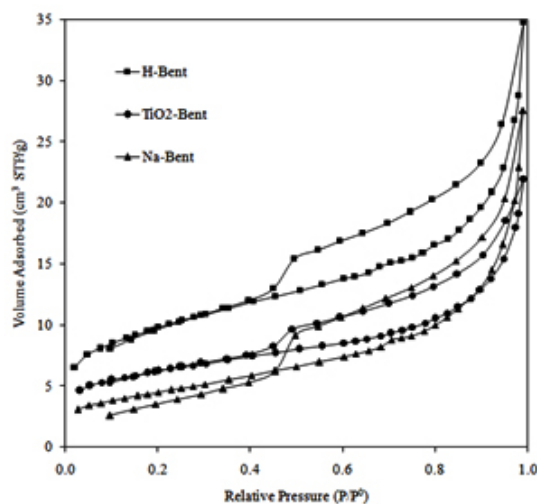


**Fig. 4: N<sub>2</sub> adsorption-desorption isotherms of Na<sub>2</sub>-bentonit, acid activated and TiO<sub>2</sub>-pillared bentonite**

values due to presence of  $H^+$  ions. At high pH values, cations are adsorbed due to the negatively charged surface sites of bentonite<sup>26</sup>.

Fig. 6 shows the dependence of adsorption of NBB on the solution pH of  $TiO_2$ -pillared bentonite at room temperature. The maximum adsorption capacity was seen at lower pH (pH ~3). As can be seen from Fig. 6, after 120 minutes the adsorption capacity of dye on  $TiO_2$ -pillared bentonite remarkably decreased from 1.202 to 0.025 mg/g with increase in pH from 3 to 11. Natural bentonite has a net negative surface charge that is balanced by exchangeable cations  $Na^+$  and  $Ca^{2+}$  at the bentonite surface. In acidic pH the  $H^+$  ions react with the bentonite surface and gave the positive charge that will be potential active site for NBB adsorption. On the other hand,

the surface charge-property of  $TiO_2$  changes with the change of solution pH due to the amphoteric behavior of semi-conductor  $TiO_2$ . The  $TiO_2$  surface is positively charged in acidic solutions and negatively charged in basic solutions. In acidic solution, adsorption of NBB primarily through the electrostatic interaction between the negative charge on dye molecules and positively charged of  $TiO_2$ . The adsorption capacity of  $TiO_2$ -pillared bentonite decreased at alkaline solution due to repulsive interaction between anionic dye molecule and negatively charged of  $TiO_2$ .

#### Effect of adsorbent dosage

Fig. 7 shows the adsorption capacity of  $TiO_2$ -pillared bentonite for the NBB at different adsorbent dosage. The adsorption capacity decrease with an increase in the adsorbent dosage. The maximum

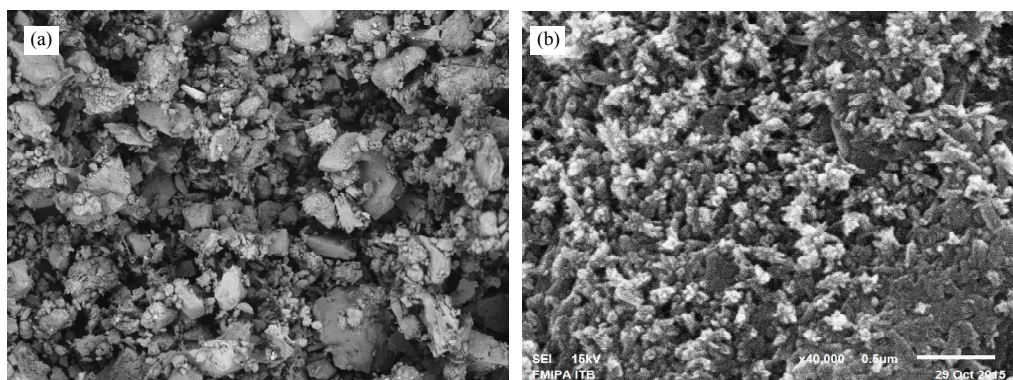


Fig. 5: SEM images of a) Natural bentonite and b)  $TiO_2$ -pillared Bentonite

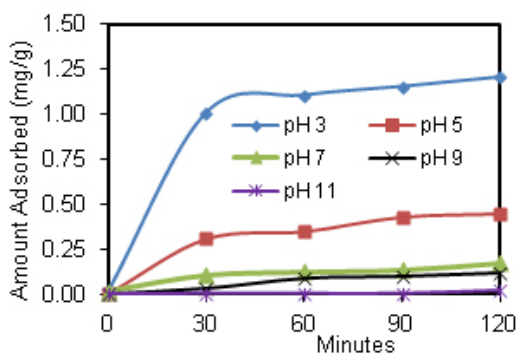


Fig. 6: Effect of pH on adsorption of NBB by  $TiO_2$ -pillared bentonite Conditions: concentration 15 mg/L and adsorbent dosage 0.2 g

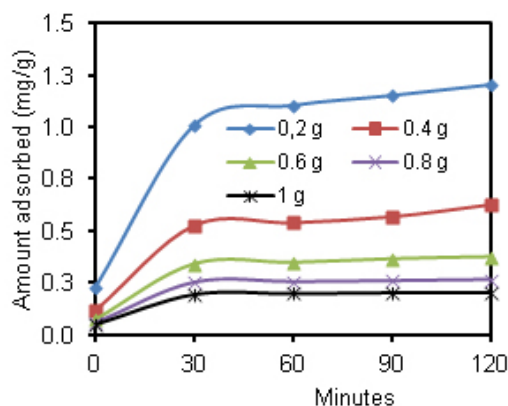


Fig. 7: Effect of adsorbent dosage on adsorption of NBB by  $TiO_2$ -pillared bentonite. Conditions: concentration 15 mg/L and pH = 3

adsorption capacity of NBB was 1.202 mg/g when 0.2 g of TiO<sub>2</sub>-pillared bentonite was used at pH = 3.

**Effect of initial dye concentration**

The effect of initial concentration of the dye solution on the adsorption is an important aspect of the study. Initial concentrations of NBB were varied in the range of 5–25 mg/L and the adsorption capacity increased with increasing initial concentration of the dye solution as shown in Figure 8.

**Comparison with natural bentonite**

The adsorption of NBB was also conducted by using natural bentonite in order to proven the

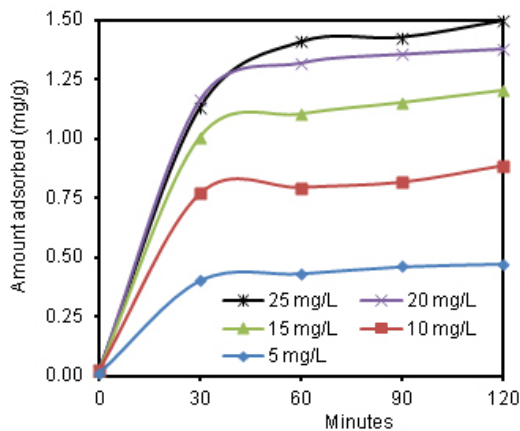


Fig. 8: Effect of initial dye concentration on adsorption of NBB by TiO<sub>2</sub>-pillared bentonite. Conditions: adsorbent dosage 0.2 g and pH 3

effect of intercalated of TiO<sub>2</sub> on bentonite interlayer. The adsorption was performed on optimum condition (pH = 3, adsorbent dosage 0.2 g and initial dye concentration 25 mg/L) which was obtained from this study (Fig. 9). The results shows that the adsorption capacity of NBB on natural bentonite (0.750 mg/g) was lower than that of on TiO<sub>2</sub>-pillared bentonite (1.496 mg/g). It can be suggested that intercalation of TiO<sub>2</sub> on interlayer of bentonite increased the adsorption capacity almost up to twice.

**Adsorption isotherms**

Adsorption isotherms are commonly used to describe the distribution of adsorbates molecules between the liquid and solid phase when the adsorption reaches an equilibrium state. Several mathematical models have been applied in equilibrium studies on dye removal by adsorption

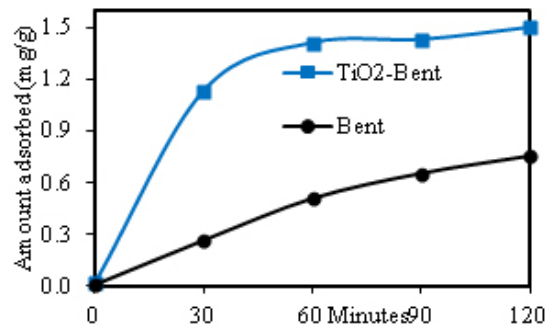


Fig. 9: Comparison of adsorption of NBB onto natural bentonite and TiO<sub>2</sub>-pillared bentonite. Conditions: adsorbent dosage 0.2 g, pH 3 and concentration 25 mg/L

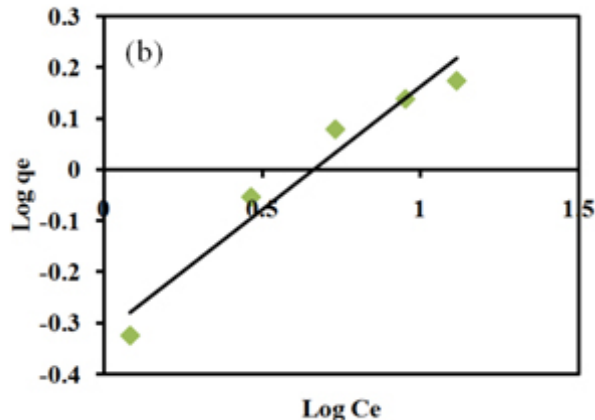
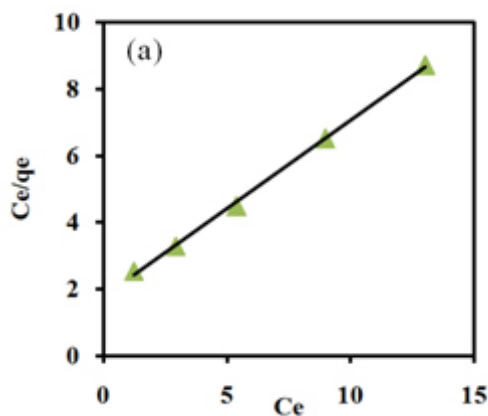


Fig. 10: Linearised form of a) Langmuir and b) Freundlich adsorption isotherm model

**Table 2: The Langmuir and Freundlich isotherm constants for NBB adsorption**

$K_L$ (L/g)	Langmuir				$r^2$	Freundlich		$r^2$
	$a_L$ (L/mg)	$Q_0$ (mg/g)	$R_L$			$K_F$ ( $\text{mg}^{1-1/n}\text{L}^{1/n}/\text{g}$ )	$n$ (g/L)	
0.080	0.560	1.901	0.392-0.617	0.998	0.479	2.0747	0.952	

onto solid surfaces. Among them, the Langmuir and Freundlich adsorption models are commonly adopted to investigate the adsorption behavior of materials and the correlation among adsorption parameters. The Langmuir isotherm model suggests that adsorption occurs on homogeneous sites within an adsorbent based on the assumption that each molecule possesses constant enthalpies and sorption activation energy. Freundlich isotherm model is generally used for multilayer adsorption between the interaction between adsorbate and adsorbent. Freundlich isotherm can be applied to non-ideal adsorption on heterogeneous surfaces<sup>29</sup>.

The adsorption data of NBB on  $\text{TiO}_2$ -pillared bentonite were analyzed according to the linear form of the Langmuir (Eq. 2) and Freundlich isotherm (Eq. 4). The values of the Langmuir constants ( $K_L$ ,  $a_L$ ,  $Q_0$ ) and Freundlich constants together with the correlation coefficient are presented in Table 2. The Langmuir and Freundlich isotherm are plotted in Fig. 10.

Fig. 10 shows the Langmuir and Freundlich isotherm was found to be linear over the entire concentration range studied with a good linear correlation coefficient ( $r^2 = 0.998$  and  $0.952$ ). The value of the correlation coefficient of Langmuir isotherm is higher than the Freundlich isotherm value showing that data correctly fit the Langmuir isotherm. It is suggested that Langmuir isotherm fits

the experimental data and confirms the monolayer coverage of NBB onto  $\text{TiO}_2$ -pillared bentonite particles and also the homogeneous distribution of active sites on the adsorbent, since the Langmuir equation assumes that the surface is homogeneous. The monolayer saturation capacity of bentonite,  $Q_0$ , was found to 1.901 mg/g.

## CONCLUSIONS

The results of present study show that  $\text{TiO}_2$ -pillared bentonite has a great potential for the removal of NBB from aqueous solution over a wide range of concentration. The initial pH, adsorbent dosage and initial dye concentration have significant effect on the adsorption of NBB on  $\text{TiO}_2$ -pillared bentonite. The optimum condition of NBB adsorption was in pH = 3, adsorbent dosage 0.2 g, initial dye concentration 25 mg/L for 120 minutes contact time. The maximum adsorption capacity reached at the optimum condition was 1.496 mg/g. The equilibrium data analyzed using Langmuir and Freundlich isotherms showed that the Langmuir isotherm provide the best correlation for adsorption of NBB onto  $\text{TiO}_2$ -pillared bentonite.

## ACKNOWLEDGEMENTS

The authors acknowledge the Ministry of Research, Technology and Higher Education of the Republic of Indonesia, for supporting this research by fundamental research project.

## REFERENCES

1. Dojcinovic, B.P.; Roglic, G.M.; Obradovic, B.M., Kuraica, M.M.; Kostic, M.M.; Nešic, J. *J. Hazard. Mater.* **2011**, *192*, 763–771.
2. Cheknane, B.; Zermane, F.; Baudu, M.; Bouras O.; Basly J.P. *J. Colloid Interface Sci.* **2012**, *381*, 158–163.
3. Çinar, O.; Yasar, S.; Kertmen, M.; Demiroz, K.; Yigit, N. O.; Kitis, M. *Process Saf. Environ.* **2008**, *86*, 455–460
4. Wu, C.H.; Chang, C.L.; Kuo, C.Y. *Dyes*

- Pigments*. **2008**, *76*, 187–194.
5. Gupta, V. K. and Suhas. *J. Environ. Manage.* **2009**, *90*, 2313–2342.
  6. Chong, M.N.; Jin, B.; Chow C.W.K.; Saint, C. *Water Res.* **2010**, *44*, 2997–3027.
  7. Gil, A.; Assis, F. C. C.; Albeniz, S.; Korili, S. A., *Chem. Eng. J.*, **2011**, *168*, 1032-1040.
  8. Crini, G. *Bioresour. Technol.* **2006**, *97*, 1061–1085.
  9. Newcombe, G. Adsorption by Carbons, **2008**, Elsevier, Amsterdam.
  10. Vimonses, V.; Lei, S.; Jin, B.; Chow, C.; Saint, C. *Appl. Clay Sci.* **2009**, *43* 465–472.
  11. Bergaya, F.; Lagaly, G., Elsevier, **2013**, . 1–19 (Chapter 1).
  12. Sen, T.K.; Gomez, D. *Desalination*, **2011**, *267*, 286–294.
  13. Xi, J.; He, M.; and Lin, C., *Microchem. J.* **2011**, *97*, 85–91.
  14. Toor, M; Jin, B., *Chem. Eng. J.* **2012**, *187*, 79– 88.
  15. Li, J.; Li, Y.; Meng, Q. *J. Hazard. Mater.* **2010**, *174*, 188–193.
  16. Ma, J.; Zhu, L. *J. Hazard. Mater.* **2006**, *136*, 982–988.
  17. Moreno-Castilla, C., *Carbon*, **2004**, *42*, 83–94.
  18. Ebie, K.; Li, F.S.; Azuma, Y.; Yuasa, A.; Hagishita, T. *Water Res.* **2001**, *35*, 167–179.
  19. Pelekani, C.; Snoeyink V.L. *Carbon* , **2001**, *39*, 25–37.
  20. Özcan A.S.; Özcan, A. *J. Colloid Interface Sci.* **2004**, *276*, 39–46.
  21. Al-Shahrani, S. S., *A. E. J.*, **2014**, *53*, 205-21.
  22. Ozacar, I.; Sengil A., *Environ. Geol.*, **2004**, *45*, 762–768.
  23. Mall, I.D.; Srivastava, V.C.; Kumar, G.V.A.; Mishra, I.M.; *Colloids Surfaces A: Physicochem. Eng. Aspects* , **2006**, *278*, 175–187.
  24. Chen, D.G.D.; Zhu, Q.; Zhou, F., , *J. Colloid Interface Sci.*, **2013**, *409*, 151-157.
  25. Sing, K. S.W.; Williams, R.T., 2004, *Adsorp. Sci. Technol.* **2004**, *22*, 773-782
  26. Bulut, E.; Ozacar M.; Sengil, A., *Microporous and Mesoporous Mater.* **2008**, *115*, 234–246.
  27. Benadjemia, M.; Millière, L.; Reinert, L.; Benderdouche, N.; Duclaux, L., *Fuel Processing Tech.* **2011**, *92*, 1203–1212
  28. Özacar, M.; Sengil, Y. A. *J. Hazard. Mater.* , **2003**, *98*, 211–224.
  29. Charalampos L.; Doulia, D.; Gimouhopoulos, K., *Sep. Purif. Rev.* **2015**, *44*: 74–107.